International Journal of Mechanical, Industrial and Aerospace Sciences
ISSN: 2517-9950
Vol:9, No:11, 2015

2D and 3D Unsteady Simulation of the Heat Transfer in the Sample during Heat Treatment by Moving Heat Source

Z. Veselý, M. Honner, J. Mach

***Abstract*—**The aim of the performed work is to establish the 2D and 3D model of direct unsteady task of sample heat treatment by moving source employing computer model on the basis of finite element method. Complex boundary condition on heat loaded sample surface is the essential feature of the task. Computer model describes heat treatment of the sample during heat source movement over the sample surface. It is started from 2D task of sample cross section as a basic model. Possibilities of extension from 2D to 3D task are discussed. The effect of the addition of third model dimension on temperature distribution in the sample is showed. Comparison of various model parameters on the sample temperatures is observed. Influence of heat source motion on the depth of material heat treatment is shown for several velocities of the movement. Presented computer model is prepared for the utilization in laser treatment of machine parts.

***Keywords*—**Computer simulation, unsteady model, heat treatment, complex boundary condition, moving heat source.

I. Introduction

MOVING heat sources, for example laser beams, are usually used during surface heat treatment. Heat source beam with certain diameter is moving over the surface in proposed tracks to influence the whole surface of the requested region.

Laser beam is partly reflected, the rest is absorbed in a small depth that is dependent on absorption coefficient of material. In the case of metals, surface absorption of heat power can be supposed.

The applications of material heating using moving heat source attract attention for many years. Analytical solution [1], [2] can be obtained under the restrictive conditions. Numerical methods for task solution are used to achieve results for more complex geometries and boundary conditions [3]-[6].

Two-dimensional numerical simulation model [7] has been developed for heat transfer during coating deposition in our laboratory. Later, this model was improved and widely used for modeling of thermal barrier coatings dynamic behaviour during thermal shocks [8]-[10]. The model was also compared with stochastic solution method [11]. Major improvement of the model has been done to enable heat transfer simulation in 3D sample geometry [12].

In this paper, the simulation model of material heat treatment using moving heat source considering 3D geometry with respect for spatial non-homogeneous profile of heat source beam is investigated.

Z. Veselý, M. Honner are with the New Technologies Research Centre, University of West Bohemia, Pilsen, CO 30614 Czech Republic (phone: 420-377-634832; fax: 420-377-634702; e-mail: zvesely@ntc.zcu.cz, honner@ntc.zcu.cz).

J. Mach was with the University of West Bohemia, Pilsen, CO 30614 Czech Republic.

The result was developed within the Centem project, reg. no. CZ.1.05/2.1.00/03.0088, cofunded by the ERDF as part of the Ministry of Education, Youth and Sports OP RDI programme and, in the follow-up sustainability stage, supported through Centem Plus (LO1402) by financial means from the Ministry of Education, Youth and Sports under the "National Sustainability Programme I.

II. Simulation Model

A. Model Characteristics

Simulation models of 2D and 3D direct unsteady tasks using finite element method are prepared. Characteristic feature of the task is complex boundary condition of heat treated sample surface. Computer model of unsteady heat transfer is created in commercial system Cosmos/M. The model describes heat treatment using moving heat source.

Sample material is supposed to be homogeneous and isotropic, initial temperature is constant in the sample volume. On the front surface of the sample, boundary condition of heat convection representing thermal effect of moving beam source heating (q_{bh}) and boundary condition of radiation cooling (q_{rc}) are used (Fig. 1 (a)). Lateral sample sides are considered thermally isolated, back side of the sample has the boundary condition of free convection cooling (q_{cc}) and radiation cooling (q_{rc}), Fig. 1 (a). Simplified two-dimensional task is solved in the sample cross-section in the *xz* plane.

Heat source moves over the sample in certain straight tracks in the *x* axis direction (Fig. 1 (b)), between the reversal points that are outside the sample. In the simple case, the beam moves over the only one track. When heat treatment fills up the larger surfaces, the beam motion in *y* axis direction (Fig. 1 (c)) is done among reversal points outside the sample. Laser beam is circular with maximum power in the centre. Power density declines with increasing distance from the beam axis.

The effect of moving heat source is described as a time and space dependent surface heat convection on the front sample surface. The basis is the heat transfer coefficient dependence on the distance from beam axis. External beam temperature (external temperature for convection) and heat transfer coefficient express heat convection as a boundary condition on the thermally loaded front sample side. The value of external temperature for convection is constant, the heat transfer coefficient is considered to be temperature independent.

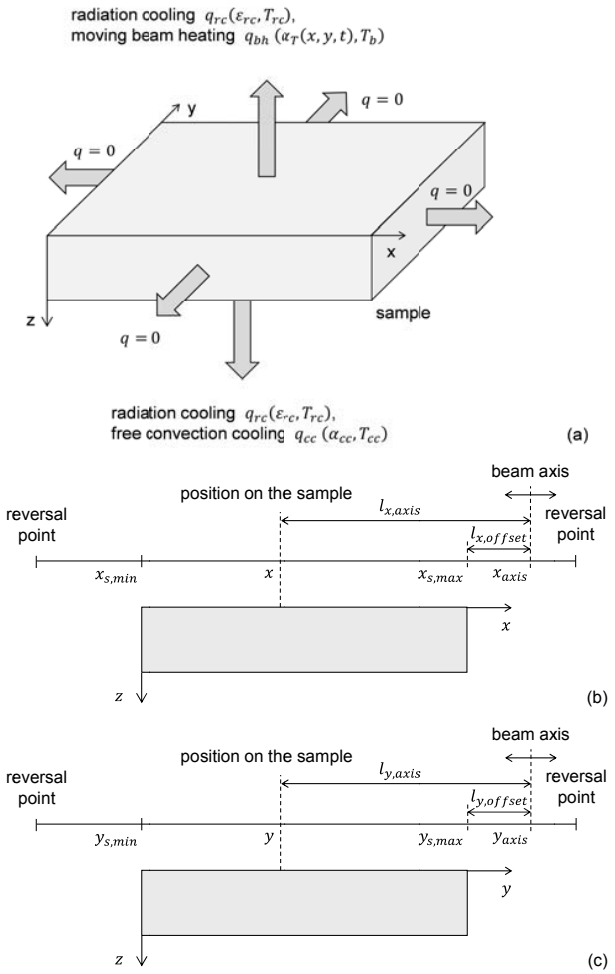

Fig. 1 Scheme of 3D model of dynamic heat treatment of the sample – geometry and boundary condition (a), heat source motion in the *x* axis (b) and *y* axis (c) directions

B. Complex Boundary Condition Definition

For the computation of time dependence of *total heat transfer coefficient* α_T for certain position (certain computational node) on the thermally loaded sample side is necessary knowledge of *basic heat transfer coefficient* α_B dependence on distance from beam axis $l_{x,axis}$ in the x axis direction, actual position of beam axis x_{axis} in the x axis direction, actual distance of beam axis from sample side $l_{x,offset}$ in the x axis direction, dependence of *reduction coefficient* $c_{\alpha,x}$ on the distance of beam axis from the sample side $x_{s,min}$ (resp. $x_{s,max}$) in the x axis direction, then the dependence of *normalized heat transfer coefficient* α_N on the distance from beam axis in the y axis direction, actual position of beam axis y_{axis} in the y axis direction, actual distance of beam axis from sample side $l_{y,offset}$ in the y axis direction, and the dependence of *reduction coefficient* $c_{\alpha,y}$ on the distance of beam axis from the sample side $y_{s,min}$ (resp. $y_{s,max}$) in the y axis direction.

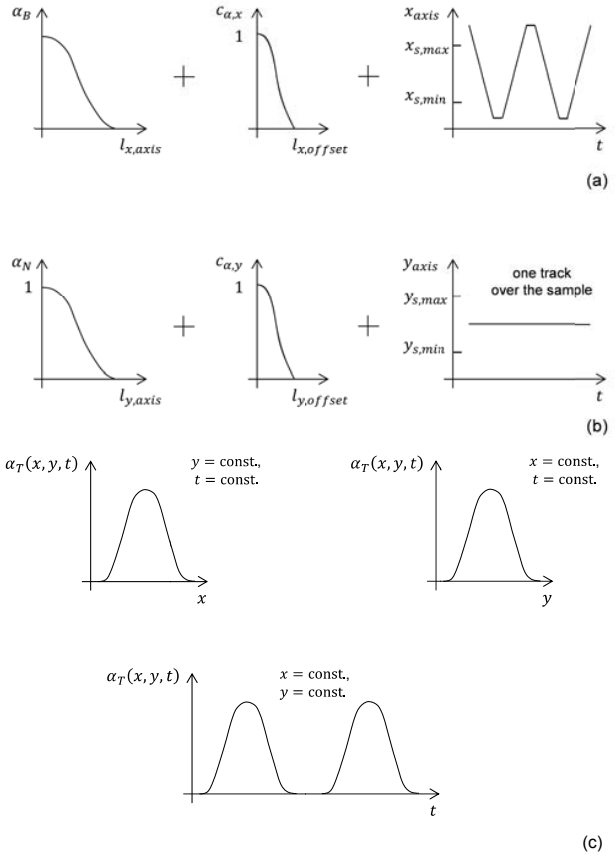

Fig. 2 Scheme of boundary condition preparation using moving heat source – input courses of quantities for 2D model (a), additive input courses for 3D model (b), output curve of total heat transfer coefficient (c)

The value of basic heat transfer coefficient α_B dependent on the distance from beam axis $l_{x,axis}$ in the x axis direction represents real space distribution of beam power. This distribution is supposed to be axially symmetric. The normalized heat transfer coefficient α_N dependent on the distance from beam axis $l_{y,axis}$ in the y axis direction is used for evaluation of boundary condition to the y axis during definition of 3D task solved as enhancement of 2D task.

Reduction coefficient $c_{\alpha,x}$ dependent on the distance of beam axis from the sample side $l_{x,offset}$ in the x axis direction towards sample neighbourhood takes into account the state when beam axis is outside the sample. Reduction coefficient is equal to one, when the beam axis is over the sample surface, and decreases with increasing distance of beam axis from sample edge. Reduction coefficient $c_{\alpha,y}$ works in the same manner in the *y* axis direction.

Characteristic courses of basic heat transfer coefficient, reduction coefficients, actual positions of beam axis, normalized heat transfer coefficient are schematically illustrated in Fig. 2 (a) (input courses for 2D model) and Fig. 2 (b) (additive input courses for 3D model). The aim is to evaluate the dependence of total heat transfer $\alpha_T(x,t)$ for 2D

model or $\alpha_T(x,y,t)$ for 3D model, Fig. 2 (c) with the scheme for 3D model. The time dependence of α_T for certain values of x, y (positions on the loaded sample side) defines heat transfer coefficient for individual computation nodes. These temporal dependencies for individual nodes can be directly loaded to computational system during simulation model preparation.

C. Mathematical Description of Boundary Condition

Equations (1)-(11) are used for full mathematical description of 3D task definition. For 2D geometry, only (1), (3), (5)-(7) are exploited. At first, total heat transfer coefficient $\alpha_T(x,t)$ in the x axis direction is determined, (1). Then in the case of 3D geometry, surface distribution of $\alpha_T(x, y, t)$ is evaluated, (2), as a boundary condition for the front side of the sample.

$$\alpha_T(x,t) = \alpha_B\left(l_{x,axis}(x,t)\right)\, c_{\alpha,x}\left(l_{x,offset}(t)\right), \quad (1)$$

$$\alpha_T(x,y,t) = \alpha_T(x,t)\,\alpha_N\left(l_{y,axis}(y,t)\right)\, c_{\alpha,y}\left(l_{y,offset}(t)\right), \quad (2)$$

where can be written

$$l_{x,axis}(x,t) = |x(t) - x_{axis}(t)|, \quad (3)$$

$$l_{y,axis}(y,t) = |y(t) - y_{axis}(t)|, \quad (4)$$

$$l_{x,offset}(t) = 0 \ldots x_{s,min} < x_{axis}(t) < x_{s,max}, \quad (5)$$

$$= |x_{s,min} - x_{axis}(t)| \ldots x_{axis}(t) < x_{s,min}, \quad (6)$$

$$= |x_{s,max} - x_{axis}(t)| \ldots x_{axis}(t) > x_{s,max}, \quad (7)$$

$$l_{y,offset}(t) = 0 \ldots y_{s,min} < y_{axis}(t) < y_{s,max}, \quad (8)$$

$$= |y_{s,min} - y_{axis}(t)| \ldots y_{axis}(t) < y_{s,min}, \quad (9)$$

$$= |y_{s,max} - y_{axis}(t)| \ldots y_{axis}(t) > y_{s,max}, \quad (10)$$

$$\alpha_N\left(l_{y,axis}(y,t)\right) = \alpha_B\left(l_{y,axis}(y,t)\right)\alpha_{B,max}^{-1}. \quad (11)$$

E. Parameters of Simulation Model

Laser source with power of $P = 4.5$ kW and beam diameter $r_b = 10$ mm is selected for simulation. Steel sample with dimensions $100 \times 70 \times 20$ mm is supposed. Laser beam motion velocities are in the range from 17.15 to 40 $\mathrm{mm.s^{-1}}$ and the distances of reversal points of laser tracks from sample edge are 10 mm. Laser beam moves along the track passing through the center of the loaded surface, motion begins at the right reversal point and finishes at the same position. Sample absorptivity a is equal to emissivity ε and emissivity for radiation cooling ε_{rc} ($a = \varepsilon = \varepsilon_{rc} = 0.7$). External temperatures for radiation and convection coolings are equal to sample initial temperature $T_{rc} = T_{cc} = T_{ini} = 20°\mathrm{C}$.

Space distribution of basic heat transfer coefficient $\alpha_B(r)$ dependent on the distance from beam axis is supposed according to Fig. 2 (a). The quantity course is described by the values $\alpha_B(r) = \alpha_{B,max}$ for $r = 0$, then $\alpha_B(r) = \alpha_{B,max}/2$ for $r = r_b/2$ and finally $\alpha_B(r) = 0$ for $r = r_b$. For the maximum of basic heat transfer coefficient holds

$$P = \varepsilon\, S_{red}\, \alpha_{B,max}\,(T_b - T_S), \quad (12)$$

where S_{red} is reduced surface of laser spot $S_{red} = \pi\, {r_{red}}^2$, $r_{red} = r_b/2$ and T_S is sample surface temperature. Beam temperature T_b is set to specific value 10 000 °C. Absolute values of basic heat transfer coefficient and specific temperature of laser beam are linked together and give the value of power P.

Several simulation models have been created in order to compare 2D and 3D task and to observe the influence of motion velocity of heat source in 3D task.

- *The comparison of 2D and 3D geometry* is carried out on the tasks with the same motion beam velocity 24 $\mathrm{mm.s^{-1}}$ (correspond to the 5 s motion time between opposites reversible points); the total process time is 10 s. The two travels of beam use the same track over the sample. The simulation results are compared to evaluate the differences between two and three dimensional models of the investigated process.
- *The comparison of heat source velocity* is provided on the 3D geometry for three velocities 17.14, 24 and 40 $\mathrm{mm.s^{-1}}$ (correspond to the 7, 5 and 3 s time of motion between opposites reversible points). The two travels of beam are conducted with the total process time 14, 10 and 7 s. The computation results are explored to evaluate the effect of various motion velocities on the sample temperatures.

III. Results

Evaluating the results from simulation models, attention is focused on sample temperature distribution and maximum temperature values in the sample.

A. The Effect of Model Dimension

The model dimension influence is compared on the time courses of the temperature in the center of the sample in various depths, and spatial courses of temperature in selected time levels.

Time courses of temperature at the center of front surface and for two depths from the surface are showed in Fig. 3. For 2D model, surface temperature after the first travel of the beam exceeds temperature required for heat treatment (800°C). After the second beam travel, surface temperature is higher than 1000°C. Maximum surface temperature 912°C is in center of the front sample surface during the first beam travel at the time 2.65 s, when the heat source has already shifted away from the surface center. During the second beam travel across the sample, temperature at center of the front surface reaches its maximum value 1027°C. The maximum of the surface temperature has been on the left side of the sample surface (1178°C), because the delay time between the subsequent beam travels over this position is the shortest and thus the temperature decrease due to heat transfer to the inside of the sample and sample surrounding is the smallest. The

maximum temperatures at the depths of 2 and 4 mm under the center of the sample front surface have been lower than 600°C.

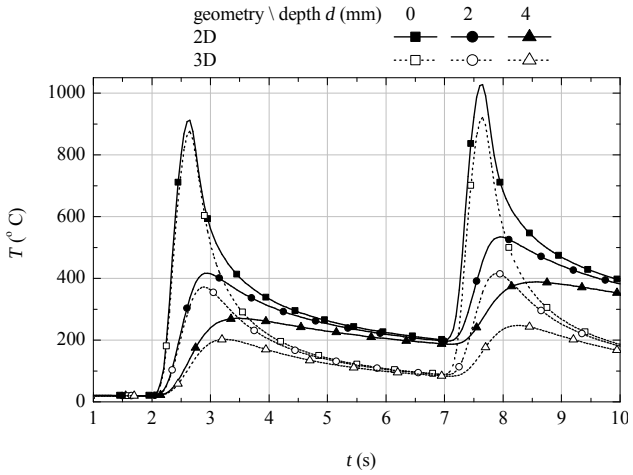

Fig. 3 Time courses of the temperature in the center of sample front surface for depths from 0 to 4 mm (x = 50 mm, y = 35 mm)

For 3D model, the temperature in the center of the sample front surface reaches 877°C at the time 2.65 s. This temperature has been about 35 °C lower compared to the 2D model, that is caused by the heat transfer in the sample to the third dimension (*y* axis). The 3D model achieves more precise results and it more resembles the reality. Maximum temperature in the centre of sample front surface during the second beam travel is 920°C.

Fig. 4 display spatial courses of the surface temperature along the beam track for 2D and 3D models. The parameter for curves is time of the process (2.5, 7.5 and 10 s). At the beginning of the process, surface temperature is equal to sample initial temperature 20°C. The laser beam is over the sample center at time 2.5 s. As can be seen on Fig. 4, maximum temperature is not in the beam spot, but several mm back against the beam motion. The left side of the beam track has still initial temperature. At time 7.5 s, when heat source is over the sample center during the second travel along the track, the maximum surface temperature is expressively higher than maximum surface temperature at 2.5 s for 2D geometry. For 3D geometry, the maximum surface temperature at time 7.5 s is only a slightly higher than at time 2.5 s. At time 10 s, surface temperature spatial course at the left part of the front surface becomes flat and the difference between 2D and 3D model is more than 200°C.

Fig. 5 presents spatial temperature courses in the *z* axis direction passing the center of sample front side for 2D and 3D models. The curves parameter is time of the process (2.5, 7.5 and 10 s). At times of 2.5 and 7.5 s, when the heat source is over the sample center, there are strong differences between 2D and 3D model. Already in the depth of 2.5 mm, there is temperature around 200°C for 3D model, meanwhile in the range 600-800 °C for the 2D model. These differences affect the sample temperatures at times, when the heat source is in reversal points. At the time 10 s, the sample surface temperature is approximately about 200 °C higher in the case of 2D model comparing to 3D model. This temperature difference is slightly increasing with increasing the positon depth, but at the depths greater than 15 mm, the differences between 2D and 3D model decreases.

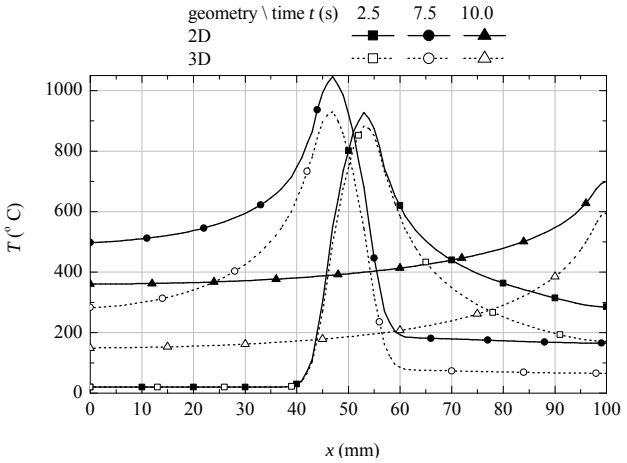

Fig. 4 Spatial courses of temperature in the *x* axis direction passing the center of sample front surface for times from 2.5 to 10 s (y = 35 mm, z = 0 mm)

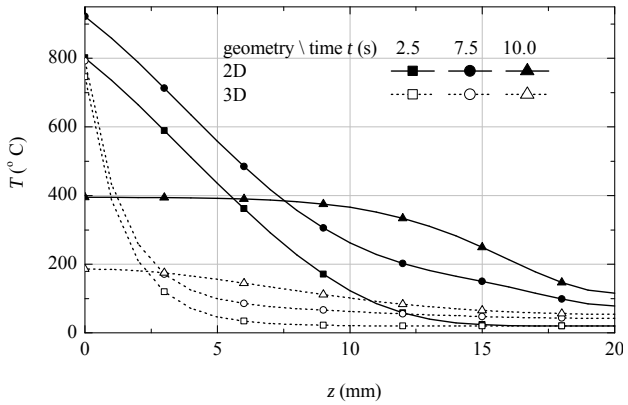

Fig. 5 Spatial courses of temperature in the *z* axis direction passing the center of the sample for times from 2.5 to 10 s (x = 50 mm, y = 35 mm)

B. The Effect of Heat Source Velocity

The sample temperature distribution dependent on beam motion velocity is observed. Total process times (two travels over the sample) 14, 10 and 7 s correspond to simulated motion velocities 17.14, 24 and 40 $mm.s^{-1}$. Because the process time depends on motion velocity, the process dimensionless time Θ is introduced; those values are in the range 0 – 1 for all cases of beam motion. Dimensionless time $\Theta = 0$ means that laser beam is in right reversal point, $\Theta = 0.5$ denotes that beam reached left reversal point and value $\Theta = 1.0$ shows laser beam to be back in right reversal point.

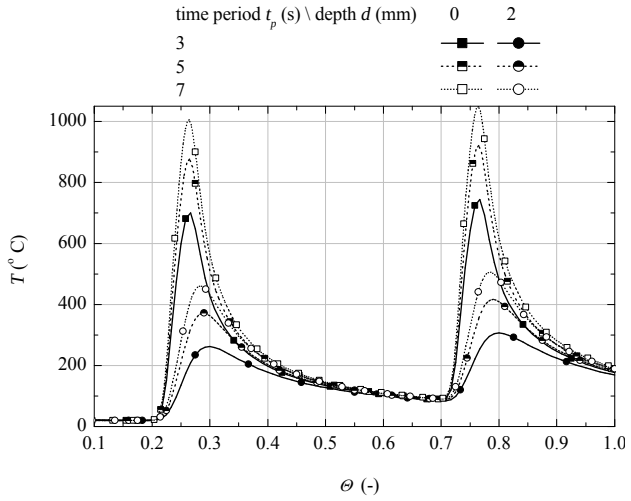

Fig. 6 Time courses of the temperature in the center of sample front surface for depths 0 and 2 mm (x = 50 mm, y = 35 mm)

Fig. 6 illustrates time courses of temperature in the centre of the front sample surface and below this position. At dimensionless times equal to 0.25 and 0.75, heat source position is over the sample center. Using motion velocity 40 mm.s^{-1}, surface temperature in the center of the track is 700 °C during the first travel of laser beam and 744°C for the second beam travel. In the case of 24 mm.s^{-1} motion velocity, the surface center temperature has its maximum 877 °C during the first beam travel, resp. 920°C during the second travel. These temperatures overpass the ones for the material heat treatment. According the assumption, taking the lowest motion velocity 17.14 mm.s^{-1}, the surface center temperature maximum is higher than in previous case. The surface center temperature maximum is 1005°C for the first, resp. 1049°C, for the second beam travel.

Fig. 7 shows spatial courses of temperature in the z direction passing the sample center. Dimensionless time is a parameter of temperature curves. At a dimensionless time $\Theta = 0.75$, the heat source is directly under the sample center during the second travel. The velocity value has a great effect on temperature spatial courses. Surface temperature is high in the range 650-900ºC, but they are rapidly decreasing with depth increase. The temperature is below 200ºC in the 3 mm depth. At a dimensionless time $\Theta = 1.0$, the heat source is back in the right reversal point. The depth temperature profile is more balanced than in the time $\Theta = 0.75$. It denotes fast temperature equalization in the sample material. The different beam motion velocity has only a small influence on spatial courses of temperature in dimensionless time $\Theta = 1.0$.

Spatial profile of surface temperature in the direction perpendicular to the beam track is in Fig. 8. The parameter of the curves is dimensionless time again. At a dimensionless time $\Theta = 0.75$, the beam is directly under the sample center during second travel. The width of heat-affected zone has only slight differences but the temperatures obtained in this zone vary for tested motion velocities. At a dimensionless time $\Theta = 1.0$, surface temperature profiles in the y axis direction gradually flatten, similarly as in the z axis direction (Fig. 7).

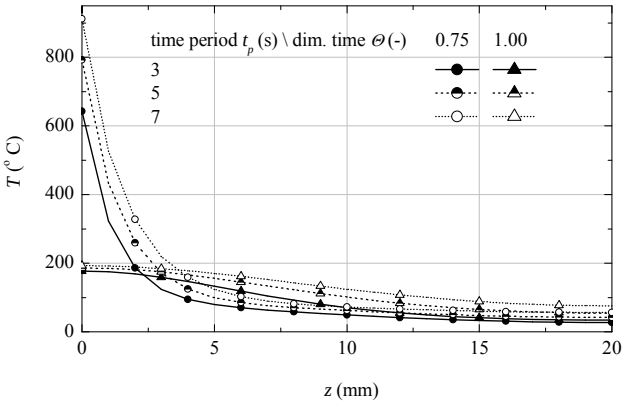

Fig. 7 Spatial courses of temperature in the z axis direction passing the center of the sample for dimensionless times 0.75 and 1.0 (x = 50 mm, y = 35 mm)

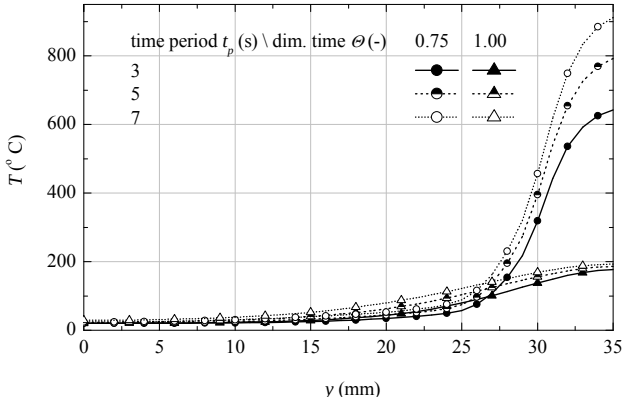

Fig. 8 Spatial courses of temperature in the y axis direction passing the center of the front sample surface for dimensionless times 0.75 and 1.0 (x = 50 mm, z = 0 mm)

C. Sample Temperature Distribution in 3D Task

Fig. 9 gives the image of spatial temperature distribution in the sample, that undergoes thermal treatment using moving heat source. There is considered beam motion velocity 24 mm.s^{-1} and figure shows the temperature state in the time 7.5 s, when the heat source is over the center of the track during the second travel.

Temperature distribution in longitudinal sample cross-section passing the track can be seen on Fig. 9 (a) (y = 35 mm). Fig. 9 (b) (z = 0 mm) illustrates surface temperature field of the sample with clearly visible beam spot. Maximum of the surface temperature at this time is about 930ºC. Transversal cross-section passing the sample center, Fig. 9 (c) (x = 50 mm), indicates the shape of the heat-affected zone in the sample.

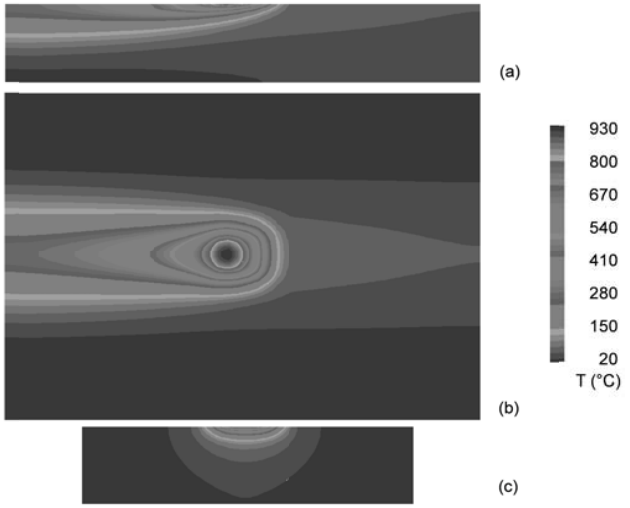

Fig. 9 Distribution of the temperature at sample front surface (b), and at longitudinal (a) and transversal (c) sample cross-sections when the heat source is in the centre of the track during the second travel

IV. Conclusion

When reviewing the 2D and 3D simulation models from the temperature distribution point of view, the lower temperature values in 3D model are evident. It is caused by the heat transfer in the *y* axis direction that is not respected in the 2D model. The temperature decrease is in the order of several tens of degrees – during the first travel of the beam over the sample, the maximum sample surface temperature in 3D model is about 35°C lower than in 2D model, and supposing second travel, the temperature reduction reaches 107°C. Involving the heat transfer in the *y* axis direction, the simulation model gives significantly more accurate results.

The effect of three beam motion velocities 40, 24 and 17.14 $mm.s^{-1}$, that correspond to the beam motion periods between the opposite reversal points 3, 5 and 7 s, on sample temperature distribution have been compared.

The motion velocity and number of beam travels over the sample have been confirmed as an important factor influencing achieved results. Lowering the beam motion velocity from 40 $mm.s^{-1}$ to 24, and 17.14 $mm.s^{-1}$, the sample surface maximum temperature increases from 700°C to 877°C, and 1005°C, during the first beam travel over the sample. Supposing second beam travel, the sample surface maximum temperature increases from 744°C to 920°C, and 1049°C. The tested motion velocities have multiple effect on surface temperature increase than addition of another beam travel over the sample. Moreover, rising the number of beam travel leads to overall sample heating that is a negative effect.

The established models of investigated process represent advantageous method of temperature field description during surface thermal treatment of materials. The knowledge of temperature distribution in particular times of the process enables further evaluation of the depths of heat-affected zone for the whole sample. Using the simulation models, it is possible to investigate the effect of process parameters (beam motion velocity, heat source power, thermal properties of processed material, etc.), or to perform process optimization, without the necessity of doing a series of experiments.

The next assumed step is to perform experimental verification of the created simulation model.

References

[1] Z.B. Hou, R. Komanduri, "General solutions for stationary/moving plane heat source problems in manufacturing and tribology", International Journal of Heat and Mass Transfer, Vol. 43, No. 10, pp. 1679-1698, 2000.

[2] P. Levin, "A general solution of 3-D quasi-steady-state problem of a moving heat source on a semi-infinite solid", Mechanics Research Communications, Vol. 35, pp. 151-157, 2008.

[3] N. Bianco, O. Manca, S. Nardini, S. Tamburino, "Transient heat conduction in solids irradiated by a moving heat source", Defect and Diffusion Forum, Vols. 283-286, pp. 358-363, Mar. 2009.

[4] S. Saedodin, M. Akbari, A Raisi, M. Torabi, "Calculation and investigation of temperature distribution and melt pool size due to a moving laser heat source using the solution of hyperbolic heat transfer equation", World Applied Sciences Journal, Vol. 11, No. 10, pp. 1273-1281, 2010.

[5] I.B. Ivanovic, A.S. Sedmak, M.V. Miloš, A.B. Živkovic, M.M. Lazic, "Numerical study of transient three-dimensional heat condition problem with a moving heat source", Thermal Science, Vol. 15, No. 1, pp. 257-266, 2011.

[6] H. Boffy, M-Ch. Baietto, P. Sainsot, A.A. Lubrecht, "Detailed modelling of a moving heat source using multigrid methods", Tribology International, Elsevier, Vol. 46, No. 1, pp. 279-287, 2012.

[7] M. Honner, P. Červený, V. Franta, F. Čejka, "Heat transfer during HVOF deposition", Surface and Coatings Technology, Vol. 106, No. 2-3, pp. 94–99, 1998.

[8] Z. Veselý, J. Kuneš, M. Honner, J. Martan, "TBC dynamic behavior during thermal shocks - simulation and experiment", in Proc. VII. Int. Conf. on Advanced Computational Methods in Heat Transfer, Halkidiki, Greece, 2002, p. 503-512.

[9] Z. Veselý, "Thermomechanical processes in heterogeneous layered structure of thermal barrier coating during thermal shock" (in Czech), Ph.D. Thesis, University of West Bohemia, Faculty of Applied Sciences, Pilsen, 171 p., 2002.

[10] J. Kuneš, Z. Veselý, M. Honner, *Thermal barriers* (in Czech). Pilsen, Czech Republic: Academia, 2003.

[11] M. Honner, J. Šroub, "Modeling of thermal spraying heat transfer processes by Exodus stochastic method", Journal of Thermal Spray Technology, Vol. 18, No. 5-6, pp. 1014-1021, 2009.

[12] J. Mach, "Modelling of thermal processes during surface laser treatment of steel" (in Czech), Diploma Thesis, University of West Bohemia, Faculty of Applied Sciences, Pilsen, 79 p., 2007.